CONSTITUTIVE MODELING OF STRESS-STRAIN CURVES OF HOT DEFORMED IF AUSTENITE

R. E. Lino
Universidade Federal de Minas Gerais. Departamento de Engenharia Metalúrgica e de Materiais.
R. Espírito Santo 35, sala 206- Centro- 30160-030- Belo Horizonte, Minas Gerais, Brazil
roneyeduardo@yahoo.com.br

R. Barbosa
Universidade Federal de Minas Gerais. Departamento de Engenharia Metalúrgica e de Materiais.
R. Espírito Santo 35, sala 206- Centro- 30160-030- Belo Horizonte, Minas Gerais, Brazil
rbarbosa@demet.ufmg.br

Abstract. *Industry forming processes such as hot rolling are complex in nature. During a rolling schedule, several process variables interact simultaneously resulting in a desired product with certain shape and mechanical properties. Setting up the rolling mill requires precise knowledge of the loads needed to shape the metal in the several passes. This in turn demands the ability to predict the strength of the material when deformed to a value of strain, strain rate and temperature. Finite element analysis is often used in pre-set models to adjust rolling mill position. They however need to be fed with constitutive equations relating the stresses required to deform a certain metal under the usual process variables. This paper shows how a set of stress-strain curves can be modeled so that both hardening and softening mechanisms commonly present during hot deformation are taken into account. The model predictions are compared to a set of literature data in order to be validated. Reasonable agreement between published results and predicted values were obtained indicating how efficient the model is to assess values of stresses under hot working.*

Keywords: *Modeling of stress-strain curves, IF steels, Hot torsion, Hot rolling*

1. Introduction

Constitutive equations relating stresses to strain rates and temperatures have been routinely employed to estimate hot forming loads (Rao and Hawbolt, 1992; Davenport et al., 2000; Jonas, 2000; McQueen and Ryan, 2002a). From all expressions published in the literature (McQueen, 2002b), probably the most used is the hyperbolic sine function relating Z, the Zener-Hollomon parameter, to the stress,

$$Z = \dot{\varepsilon} \exp\left(Q_{def} / RT\right) = A\left(sinh\alpha\sigma\right)^{n} \tag{1}$$

Here, Q_{def} is the activation energy for hot deformation, A, α and n are constants, the other symbols have their usual meaning. This expression gives a straight line in a log Z versus log[sinh(ασ)] plot irrespective of the level of the stresses, whereas the power and exponential laws loose linearity at high and low stresses respectively. The peak stress resulting from the occurrence of dynamic recrystallization, DRX, and also the steady state stress associated with the completion of first wave DRX, have been successfully modeled by the above expression. Q_{def} can also be estimated for a series of C-Mn and microalloyed steels as a function of chemical composition, as published in the literature (Cho et al., 2001).

Modeling stress strain curve requires, in addition, the use of an evolution equation such as forwarded by Sellars (1985). The purpose of this paper is therefore twofold; first, to simulate isothermal stress strain curves during hot deformation of double stabilized Ti-Nb IF steel, following the method proposed by Sellars and, second to predict values of stresses during continuous cooling as it occurs in hot rolling.

2. Experimental Procedure

The chemical composition of the IF steel used in this work is 24ppmC, 9ppmN and 1.70Mn, 0.17Si, 0.006P, 0.002S, 0.021Al, 0.014Ti and 0.11Nb, all numbers in weight%. Samples for torsion experiments, 15mm of length and 10mm in diameter, were cut at ¼ of the thickness of a hot rolled billet of $100mm^2$ cross section. The specimens were machined with their axis parallel to the billet rolling direction. The experiments were carried out in a computer controlled servo-hydraulic machine equipped with an infrared furnace. All tests were performed in argon atmosphere and the temperature was controlled by a cromel-alumel thermocouple welded at the sample surface. The specimens were initially pre-heated at 1473K (1200^{o}C) for 900s (15 minutes). Torque and angular displacement were converted to equivalent stress-strain curves in the usual way (Fields and Backofen, 1957).

Non-isothermal testing was conducted to determine the values of Tnr and Ar3, as reported elsewhere (Borato et al., 1988). The samples were pre-heated as just described and let to cool at a rate of 1K/s (1°C/s). Deformations of 0.3 equivalent strains were applied to the sample at time intervals of 30s. The first deformation was given at approximately 1453K (1180°C) and the last at about 873K (600°C), covering temperatures typical of hot rolling in the austenite and a reasonable range of temperatures in the ferrite region. The values of Tnr and Ar3 measured were 1218K (945°C) and 1023K (750°C), respectively.

Isothermal testing was performed to obtain stress-strain curves at constant strain rate and at several temperatures. Samples were pre-heated as described above and then let to cool to testing temperature at a rate of 1K/s (1°C/s). All samples were kept at 90s (3 minutes) prior to twisting promoting temperature equalization throughout the specimen before deformation, except for the case of tests conducted at 1473K (1200°C). Tests were performed at temperatures of 1123, 1173, 1223, 1273, 1323 and 1373K (850, 900, 950, 1000, 1050 and 1100°C) and strain rates of 0.1, 1, 3 and $10s^{-1}$. All samples were deformed to an equivalent true strain of 7, allowing the occurrence of full DRX and the achievement of the steady state in all tests.

3. Results and discussion

3.1. Modeling isothermal stress-strain curves

Figure 1 shows, as full lines, the measured stress-strain curves for samples tested at a strain rate of $1s^{-1}$ and temperatures ranging from 1173 to 137K (900 to 1100°C). All curves display a characteristic peak stress, ε_p, indicating occurrence of DRX. The specimens were purposely deformed to total strains around 7.0 in order to guarantee full DRX even at the lowest temperature. The circles in Fig. 1 represent calculated values giving a qualitative view of how well the model presented here can simulate isothermal stress-strain curves.

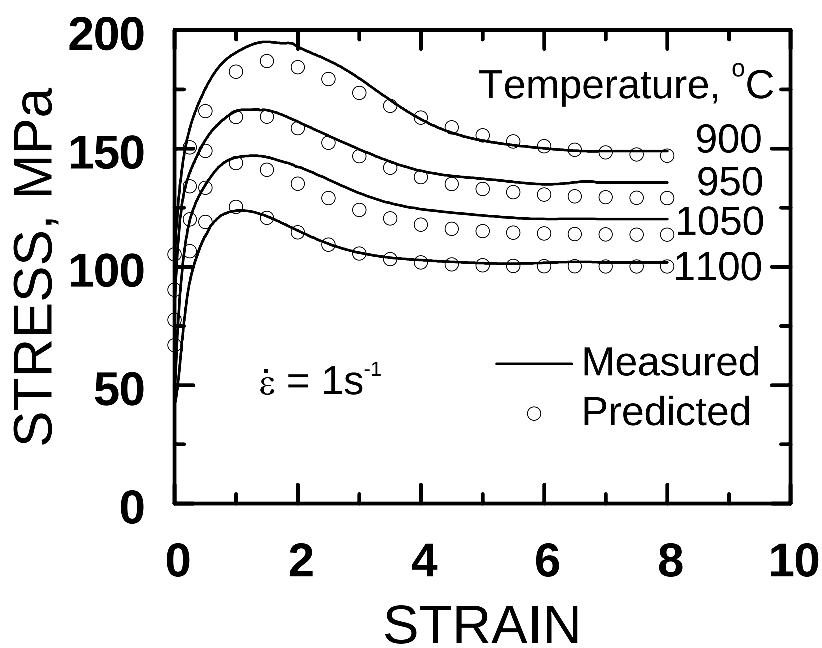

Figure 1. Comparison between measured and predicted stress-strain curves for tests conducted at $1s^{-1}$ and several temperatures.

Table 1 presents a summary of the equations employed in this work to model the stress-strain curves. The dependence on Z of the stress at constant strain is given by the sinh law, as shown by Eq. (1) and the activation energy for hot deformation was estimated from log [sinh ($\alpha\sigma$)] versus log (1/T), at constant strain rate, taking α as 0.012 MPa^{-1}, as suggested in the literature (McQueen, 2002b) for several steels and n was calculated for a given temperature from the slopes of log (sinh ($\alpha\sigma$)) versus log (ε) plots. The values of Q_{def} and n measured in this work were 305 ± 12kJ/mol and

4.8 ± 0.2, respectively. These values compare favorably to 302kJ/mol and 4.5, the former calculated from expression reported in the literature (Medina and Hernandez, 1996).

The critical strain for the initiation of dynamic recrystallization, ε_c, given by Eq. (3) and (4), is of importance since it determines the correct set of equations to be used as a function of the strain. This critical value was measured from the stress-strain curves following a method presented by Poliak and Jonas (Poliak and Jonas, 2003). For strains lower than ε_c the stresses were calculated using Eq. (5). All the symbols in this expression have their usual meaning, except for C, a function of the initial curvature of the stress-strain curve, as represented by the stress at a constant strain for a given Z, in this case, half the value of the peak strain. The constant m in Eq. (5) was measured as 0.5 ± 0.1, in agreement with reported value derived from more fundamentally based models. At the initiation of the steady state stress, Eq (5) will produce a saturation stress, σ_e, given by the expression in Eq. (7). This stress is a function of Z and its measurement for each Z value was carried out following method recently published in the literature (Zahiri et al. 2005) For strains higher than ε_c, softening by DRX was taken into account in the modeling of the curves as shown by Eq. (8). The kinetics of DRX cannot be measured directly from metallography observation on quenched samples of IF steels since austenite transforms on cooling to ferrite, irrespective of the cooling rate employed. Therefore, DRX was measured from the shape of the stress-strain curves, as reported in the literature (Sellars, 1985). The kinetics of DRX follows, as expected, an Avrami type expression and the time exponent measured here was m´ equals 1.4 ± 0.1.

Table 1. List of equations employed in this work to simulate isothermal stress-strain curves of Ti-Nb IF steel.

Event	Equation
Zener-Hollomon parameter	$Z = \dot{\varepsilon}\exp[Q/(RT)]$ $Q = (305 \pm 12)kJ/(molK)$ (2)
Critical strain for the initiation of dynamic recrystallization	$\varepsilon_c = a\varepsilon_p$ $a = 0.6 \pm 0.1\,(measured)$ (3) $\varepsilon_p = 1.03x10^{-2} Z^{0.16}$ (4)
Stress at a constant Z in the dynamic recovery region ($\varepsilon < \varepsilon_c$)	$\sigma = \sigma_0 + (\sigma_e - \sigma_0)[1 - \exp(-C\varepsilon)]^m$ $m = 0.5 \pm 0.1\,(measured)$ (5 $C = \frac{1}{\varepsilon_x}\ln\left[1 - \left[\frac{\sigma_{\varepsilon_x} - \sigma_0}{\sigma_e - \sigma_0}\right]^{1/m}\right]$ (6) $\varepsilon_x = \varepsilon_p / 2$ $\sigma_0 = 83\sinh^{-1}\left[Z/2.2x10^{12}\right]^{0.2}$ $\sigma_e = 83\sinh^{-1}\left[Z/1.3x10^{10}\right]^{0.2}$ (7) $\sigma_{\varepsilon_x} = 83\sinh^{-1}\left[Z/5.6x10^{10}\right]^{0.2}$
Stress at constant Z in the dynamic recovery and dynamic recrystallization region ($\varepsilon \geq \varepsilon_c$).	$\sigma = \left\{\sigma_0 + (\sigma_e - \sigma_0)[1 - \exp(-C\varepsilon)]^m\right\} - \Delta\sigma$ $\Delta\sigma = (\sigma_e - \sigma_{ss})\left\{1 - \exp\left[-k((\varepsilon - \varepsilon_c)/\dot{\varepsilon})^{m'}\right]\right\}$ (8) $m' = 1.4 \pm 0.1\,(measured)$ $k = 246\dot{\varepsilon}^{1.5}\exp\left[67x10^3/(RT)\right]$ $\sigma_{ss} = 83\sinh^{-1}\left[Z/3{,}2x10^{11}\right]^{0.2}$ (9)

3.2. Modeling stress-strain curves during continuous cooling at temperatures higher than Tnr

Equations presented here can simulate isothermal stress-strain curves for the present chemical composition of IF steel, as just described. In addition, if coupled with a suitable model, they can also be employed to estimate rolling loads. Literature data on rolling loads, usually represented as a function of a mean flow stress (MFS), although abundant for C-Mn and Nb microalloyed steels, are relatively scarce for IF steels. For this reason, in order to compare predictions of the present model with stress-strain curves measured during continuous cooling, this paper refers to data published by Najafi-Zadeh et al. (1992) to validate the work carried out here. These authors used three types of IF steels: Ti, Ti-Nb and Nb. They performed two types of torsion tests: one to measure Tnr and a second type to simulate a hot strip rolling process. In their work, the Ti and the Ti-Nb steels displayed equivalent levels of MFS when subjected to similar schedules. The Nb IF steel, however, displayed significantly higher values of MFSs suggesting that Nb increased pronouncedly the strength levels of the steel. It was also shown that Tnr occurred whenever Nb was present, this values being around 1213 to 1233K (940 to 960^{o}C). At temperatures above Tnr, there was, as expected, full recrystallization between deformation, whereas below Tnr there was an accumulation of strain from pass to pass triggering DRX in the second deformation and displaying a drop in the MFS value of the following pass.

Figure 2 shows a comparison between MFS calculated from the present model and the values reported in the paper just cited for passes given at temperatures higher than Tnr, that is, in the full recrystallization region. Clearly, the predicted values are consistently higher than those reported in the literature by about 30%, although the shape of the calculated MFS versus 1000/T curve was identical to the curve presented in the literature. This discrepancy, however, can be accounted for if differences in chemical composition between alloys, the one used to obtain the data presented in the literature and that employed here, are considered. In fact, the alloy used in the comparison shown in Fig. 2 and employed by Najafi-Zadeh, Yue and Jonas had 0.15% Mn, 0.035% Ti and 0.028% Nb whereas the alloy used here has 1.71% Mn, 0.014 Ti and 0.11% Nb. Clearly, the presence of 10 times more Mn and 5 times more Nb in the alloy tested here affected the overall strength of the samples deformed in this work. In order to assess the effect of these differences on the values of MFS an expression reported by Siciliano et al. (1996), was used.

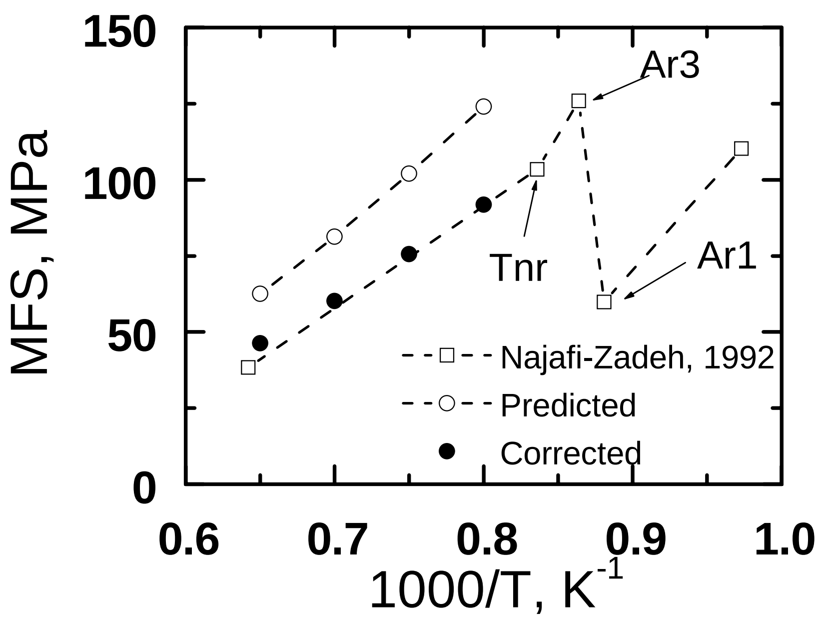

Figure 2. Comparison between predicted mean stress values calculated using the model presented in this work and experimental data available in the literature (Najafi-Zadeh et al., 1992) during continuous cooling and deformations given at temperatures higher than Tnr.

$$MFS = \sigma_M (0.768 + 0.51[Nb] + 0.137[Mn] + 4.217[Ti]) \quad (10)$$

Here, σ_M stands for a flow stress calculated according to Misaka (Siciliano, Jr., 1996). The value of σ_M depends on C content, strain and strain rate and, as C content for the steel tested by Najafi-Zadeh, Yue and Jonas is of the same order of the one for the steel tested here, the values of stresses calculated from Misaka´s equation produced similar values in both cases. Therefore, a “correction” factor could be calculated from the part of Eq. (10) within the parenthesis. This part of the equation predicts a factor of 0.797 for the Ti-Nb steel used by Najafi-Zadeh, Yue and Jonas and of 1.048 for the present work, if it is taken into the expression the % weights of Ti and Nb in excess to stabilize C and N in the IF matrix and not the gross nominal composition. The amount of Ti or Nb in excess was obtained by subtracting from the base composition the amount Ti or Nb combined with N, S or C, as detailed elsewhere (Najafi-Zadeh, 1992). Hence, the strengthening factor due to different amounts of Ti and Nb in excess to stabilize C and N in both alloys is 1.048/0.797 or 1,310, close to the 30% difference found here. This correction factor was then applied to compare the MFSs of the two alloys, showing an agreement between calculated and literature results as depicted by the black circles in Fig. 2.

The agreement between measured and predicted values just shown validates the use of present model to predict stresses at temperature ranges higher than Tnr. At temperatures lower than Tnr, however, further study must be carried out concerning the kinetics of dynamic and metadynamic softening prior to the usage of the Eqs. presented in Table (1) and, clearly, it is out of the scope of such short note, being the subject, nonetheless, addressed in a separate cover.

4. Conclusions

The following conclusions can be drawn from this work:

A simple model was presented here to predict isothermal stress-strain curves of a Ti-Nb IF steel. The results have shown that the model can be used to compute isothermal stress-strain curves being the agreement between measured and predicted stresses reasonable, regardless of the level of the strain, weather smaller or larger than ε_c, and the values of strain rate and temperature at which the test was conducted;

The model was validated by comparing values of MFS calculated here with those reported by Najafi-Zadeh et al. (1992) at temperatures higher than Tnr during continuous cooling experiments simulating the roughing stage of hot rolling of plates and strips. The predicted MFS values were systematically higher by a factor of about 30% than the data reported in the literature. These discrepancies, however, were related to differences in chemical composition regarding Mn, Ti and Nb contents in both alloys. Once differences in chemistry were properly taken into consideration, measured and predicted values of MFS could be appropriately compared.

5. Acknowledgments

The authors acknowledge CNPq and PRPq-UFMG for the financial support given to this research.

6. References

Borato, F., Barbosa, R., Yue, S. and Jonas, J. J., 1988, "Effect of Chemical Composition on the Critical Temperature of Microalloyed Steels", Proceedings on the Int. Conf. Physical Metallurgy of Thermomechanical Processing of Steels and Other Metals (THERMEC '88), Vol. 1, Tokyo, Japan, pp. 383-390.

Cho, S-H., Kang, K. B. and Jonas, J. J., 2001, "Mathematical Modeling of the Recrystallization Kinetics of Nb Microalloyed Steels" ISIJ International, Vol. 41, pp. 766-773.

Davenport, S.B., Silk, N.J., Sparks, C.N. and Sellars, C.M., 2000, "Development of constitutive equations for modelling of hot rolling", Materials Science and Technology, Vol. 16, pp. 539-547.

Fields, D.S. and Backofen, W. A., 1957, "Determination of strain-hardening characteristics by torsion testing", American Society for Testing and Materials, Vol. 57, pp. 1259-1272.

Jonas, J.J., 2000, "The hot strip mill as an experimental tool", ISIJ International, Vol.40, pp. 731-738.

McQueen, H. and. Ryan, N.D., 2002, "Constitutive analysis in hot working", Materials Science and Engineering A, Vol. A322, pp. 43-63.

McQueen, H., 2002b, "Elevated temperature deformation at forming rates of 10^{-2} to $10^{2}s^{-1}$", Metallurgical and Materials Transactions A, Vol. 33, pp. 345-363.

Medina, S.F. and Hernandez, C.A., 1996, "The influence of chemical composition on peak strain of deformed austenite in low alloy and microalloyed steels", Acta Materialia, Vol. 44, pp. 137-154.

Najafi-Zadeh, A.; Yue, S. and Jonas, J.J., 1992, "Influence of hot strip rolling parameters on austenite recrystallization in intersticial free steels", ISIJ International, Vol. 32. n. 2, pp.213-221.

Poliak, E. I. And Jonas, J.J., 2003, "Initiation of Dynamic Recrystallization in Constant Strain Rate Hot Deformation", ISIJ International, Vol. 43. pp. 684-691.

Zahari, S.H., Davies, C.H.J. and Hodgson, P.D., 2005, "A mechanical approach to quantify dynamic recrystallization in polycrystalline metals", Scripta Materialia, Vol. 52, pp. 299-304.

7. Responsibility notice

The authors are the only responsible for the printed material included in this paper.